J. Fluid Mech. (1991), *vol.* 229, *pp.* 499–516
Printed in Great Britain

Direct simulation of turbulent spots in plane Couette flow

By ANDERS LUNDBLADH† AND ARNE V. JOHANSSON
Department of Mechanics, Royal Institute of Technology, S-100 44 Stockholm, Sweden

(Received 30 May 1990 and in revised form 2 February 1991)

The development of turbulent spots in plane Couette flow was studied by means of direct numerical simulation. The Reynolds number was varied between 300 and 1500 (based on half the velocity difference between the two surfaces and half the gap width) in order to determine the lowest possible Reynolds number for which localized turbulent regions can persist, i.e. a *critical* Reynolds number, and to determine basic characteristics of the spot in plane Couette flow. It was found that spots can be sustained for Reynolds numbers above approximately 375 and that the shape is elliptical with a streamwise elongation that is more accentuated for high Reynolds numbers. At large times though there appears to be a slow approach towards a circular spot shape. Various other features of this spot suggest that it may be classified as an interesting intermediate case between the Poiseuille and boundary-layer spots. In the absence of experiments for this case the present results represent a true prediction of the physical situation.

1. Introduction

Investigations of transition to turbulence in laminar shear flows have traditionally been focused on the growth and breakdown of disturbances describable in terms of the least-stable two-dimensional Tollmien–Schlichting mode alone, or (at finite amplitude) together with superimposed oblique waves. It has been shown both experimentally and theoretically that three-dimensionality is essential in this breakdown process, which now also has been simulated numerically by Spalart & Yang (1987) and Gilbert (1988). Transition to turbulence through breakdown of spatially localized disturbances, which hence must be described in terms of a number of eigenmodes, has received less attention, at least from the theoretical point of view.

The evolution of localized disturbances, in Poiseuille and boundary-layer flows, has been analysed by use of direct numerical simulation techniques by Henningson, Johansson & Lundbladh (1989) and Breuer (1989), respectively. In those investigations the evolution was followed up to the early stages of breakdown of the laminar flow. The rate at which this occurs is of course highly amplitude-dependent. However, the final result of the breakdown of a localized disturbance is a localized growing region of turbulence, i.e. a turbulent spot, that exhibits a considerable degree of universality of the overall characteristics.

The interior structure of such a turbulent spot and, in particular, the mechanisms responsible for its rapid growth have been key issues of interest in a number of experimental investigations. For a review of this work see e.g. Riley & Gad-el-Hak (1985). The spot development in the boundary-layer and channel geometries has now also been simulated numerically (Henningson, Spalart & Kim 1987).

† Also at: FFA, PO Box 11021, S-161 11 Bromma, Sweden.

Plane Couette flow represents one of the fundamental, canonical, flow situations that has attracted much attention in terms of theoretical studies of stability and transition mechanisms. The lack of curvature of the velocity profile simplifies the equations significantly, and a large number of studies have, since the early part of this century, addressed the problem of linear stability of Couette flow (see e.g. Gallagher 1974). It is now known to be linearly stable and several studies have also addressed problems associated with its nonlinear stability characteristics (see e.g. Ellingsen, Gjevik & Palm 1970). Orszag & Kells (1980) carried out two- and three-dimensional calculations with a pseudospectral technique. They found two-dimensional disturbances to remain stable even at quite large amplitudes and high Reynolds numbers, in contrast to the stability calculations of Ellingsen *et al.* However, when small-amplitude oblique waves were superimposed on a finite-amplitude two-dimensional wave, their growth and the subsequent breakdown of the flow was found to occur in a similar manner and at comparable Reynolds numbers as for plane Poiseuille flow. They observed transition to turbulence in three-dimensional calculations (with $16 \times 33 \times 16$ modes) at a Reynolds number, based on half-channel width and half the difference in velocity between the two surfaces, of 1250. Owing to spatial resolution effects they were not really able to carry the computations into the regime beyond initial breakdown.

Recently, Nagata (1990) has made a numerical investigation of the nonlinear stability of plane Couette flow. He found finite-amplitude steady-state solutions at a Reynolds number of around 125, defined as above (by his definition 500). The resolution is extremely low in that at most 13 expansion modes are used in the vertical direction, although the results show a tendency to converge. Furthermore, no stability analysis of the steady-state solutions has been performed. If the solutions were to prove unstable they could not be realized in practice and no clear conclusions of the transitional Reynolds number for the flow can be drawn. In view of this and the discrepancy with experiments (cf. below) the importance of these solutions is doubtful.

Experimental investigations of plane Couette flow are associated with particular difficulties, and are hence scarce. No study of turbulent spots in this situation has been carried out. Experiments at transitional Reynolds numbers have been carried out by Reichardt (1956) in an oil channel and Leutheusser & Chu (1971) in an air flow between a stationary wall and a moving water surface. The *critical* Reynolds number, determined as that below which no turbulent fluctuations were observed, was found to be about 750 by Reichardt, whereas Leutheusser & Chu obtained a considerably lower value of about 280. The discrepancy may possibly be explained by the rather small aspect ratio (5) used in the former study (12 in the latter), and differences in inlet disturbance level.

In the present study direct numerical simulations of the Navier–Stokes equations are used to study the development of turbulent spots in plane Couette flow over a range of Reynolds numbers. The lowest Reynolds number for which spots can be sustained is determined within a narrow interval. The value determined in this way represents a rather well-defined critical (or transition) Reynolds number. Also other characteristics of the spot, such as its shape and spreading rates are determined for various Reynolds numbers, and since no experiments exist today comparisons with measured data are not possible yet.

2. Numerical method

The simulation code used for the present computations uses spectral methods to solve the Navier–Stokes equations, with Fourier representation in the streamwise (x) and spanwise (z) directions, and Chebyshev polynomials in the wall-normal (y) direction. The nonlinear terms are treated pseudospectrally using FFT's, in a manner similar to that of Kim, Moin & Moser (1987). Instead of the variables themselves, their second derivatives are expanded in Chebyshev series. This results in a better conditioned problem (see Greengaard 1988), and yields an easy method of obtaining a consistent truncation of the expansions, thus giving better numerical accuracy. The program is written to be as portable between different machines as possible. Its performance has been verified in various ways, such as through computation of growth (and decay) rates for two-dimensional and oblique Tollmien–Schlichting waves in Poiseuille flow at various Reynolds numbers. It was also used to analyse the development of localized disturbances in plane Poiseuille flow (Henningson *et al.* 1989).

For the bulk of the calculations the size of the computational domain was $128 \times 2 \times 64$ in the streamwise, wall-normal and spanwise directions, respectively, although symmetry with respect to the mid (x, y)-plane was imposed. The surface velocities were taken as $\pm U_0$. If not explicitly stated otherwise, all quantities will be non-dimensionalized using the half-channel height, h, and U_0. They were discretized using $256 \times 33 \times 256$ spectral modes for the computations at Reynolds numbers ($Re = U_0 h/\nu$) up to 750.

The computations at $Re = 750$ were continued to large times by use of a larger box ($256 \times 2 \times 128$) for times between 90 and 160. The number of modes in the x- and z-directions was also doubled to retain the same spatial resolution as for earlier times. The technique to minimize artificial effects in connection with the change of box size at $t = 90$ was as follows. First the u and v fields were extended periodically in the larger box. A pointwise multiplication by a window function that is flat and equal to unity in the central region, and decaying exponentially towards the box edges, was then applied. The w component was thereafter obtained by use of the continuity equation. For comparison, the computation with the smaller box was continued to $t = 100$. Plots for that time from the two computations showed no visible differences except very near the box edges.

For $Re = 1500$ the number of modes in the y-direction was doubled and the box had a horizontal extent of 90×40 in order to keep the spatial resolution at nearly the same level as for $Re = 750$ in terms of wall units, and still allow computation of the spot development up to a non-dimensional time, t, of 50.

As an illustration of the spatial resolution achieved, one-dimensional energy spectra of u at the centreline ($y = 0$) are shown in figure 1 for $Re = 750$. Similar results were obtained at other y-locations, and the drop at high wavenumbers for v is slightly less than that in figure 1. The resolution in the y-direction was substantially better than in the horizontal directions. More pertinent tests of the spatial resolution is actually obtained from grid refinements. The spatial resolution problem is always an important one in simulations of turbulent flows. Some more details on this issue will therefore be given in connection with the presentation of the results, in order to verify that the spatial resolution was sufficient.

In order to test the sensitivity of the spot growth characteristics to the specifics of the initial disturbance in general, and to the imposed symmetry in particular, a computation was carried out without this constraint for an initial disturbance that

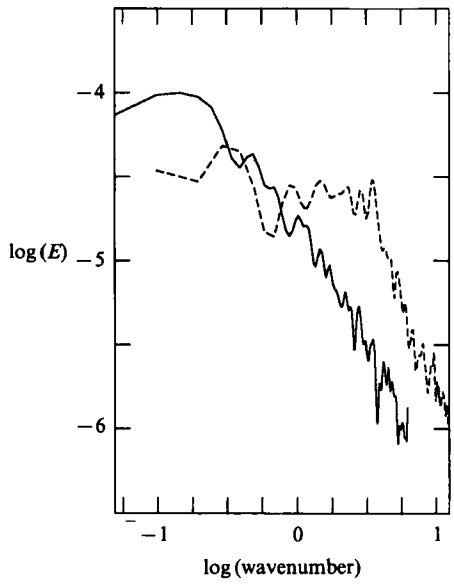

FIGURE 1. One-dimensional energy spectra of u ($t = 50$, $Re = 750$) as function of streamwise (solid curve) and spanwise (dashed curve) wavenumber.

lacked the symmetry about the plane $z = 0$. The effective spatial resolution was the same as for the symmetric computations.

A time-step of 0.025 (0.01 for $Re = 1500$) was used for most of the computations, resulting in a CFL number at about half the empirical stability limit.

The computations, including tests with other discretizations not reported in detail here, totalled more than 400 CPU hours on a CRAY XMP48 machine. The CPU-time required per mode and time-step was 11 μs.

3. Results

The spots were triggered by an initial disturbance consisting of four pairs of counter-rotating vortices with axes of rotation that, for the bulk of the computations, were aligned with the x-direction, thus giving an initial disturbance symmetric with respect to the $z = 0$ plane. Since an initial symmetry of this kind is preserved by the Navier–Stokes equations, even for finite-amplitude disturbances, advantage was taken of this feature to reduce the computational effort by imposing spanwise symmetry in the calculations. The initial disturbance with spanwise symmetry can be described in the form

$$\psi = Ay(1-y^2)^2 xz\, e^{-x^2-z^2}, \qquad v = \psi_z, \quad \omega = -\psi_y,$$

where (u, v, w) are the streamwise, normal, and spanwise velocities. Note that the initial u-disturbance here is identically zero. The amplitude coefficient A was chosen such that the maximum initial v was 0.6, and the form of the y-polynomial is such that both symmetric and antisymmetric parts are excited (and boundary conditions satisfied). Here, symmetry is defined as invariance to 180° rotation around the line $x = 0$, $y = 0$. The *effective* initial extents of the x- and z-directions are a few channel heights. The initial amplitude and initial energy were, hence, chosen to be quite large in order to obtain results valid in the limit of *very strong* disturbances. It is known

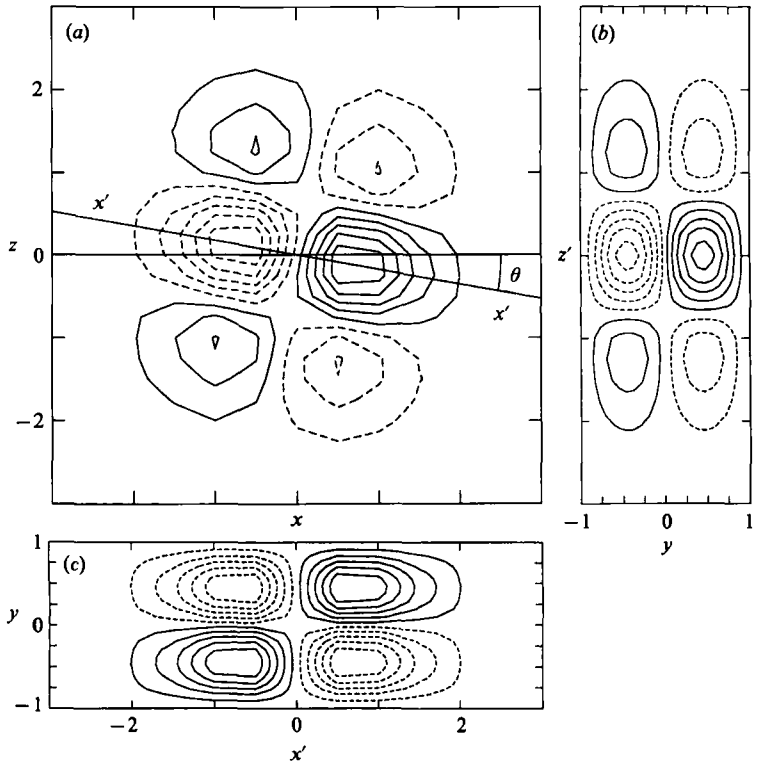

FIGURE 2. The initial disturbance ($\theta = 0$ for symmetric cases). Contours of v starting at -0.45 with increments of 0.1 are shown. (*a*) $y = 0.47$, (*b*) $x' = 1.0$, (*c*) $z' = 0$.

from experimental investigations of spots in various types of flows that the spot characteristics become essentially independent of the specifics of the initial disturbance for strong enough disturbances. The test run with an initial disturbance without the spanwise symmetry was achieved by rotating the disturbance, described above, by 10° around the $x = 0$, $z = 0$ line (see figure 2).

The evolution of the initial disturbance into a growing region of turbulence at Reynolds numbers between 300 and 1500 is shown in figure 3. The development is shown up to $t = 90$ except for the highest Reynolds number for which times up to 50 are shown. Here ± 0.02 contours of v at the centreline ($y = 0$) are chosen to depict the spreading of the spot. The boundary between laminar and turbulent flow is quite distinct and relatively independent of the actual choice of contour level. It should be noted that the centre remains at the same location since the two surfaces have velocities of equal magnitude but opposite sign. At $Re = 300$ the disturbed region grows initially, but the amplitudes and total energy decay, and the v-levels have fallen below 0.02 at $t \approx 60$. The u-disturbance decays more slowly, but at large times the remaining u-disturbance consists merely of long longitudinal streaks of alternating low and high velocity, which are dominated by one specific spanwise wavelength (approximately 3.2).

At $Re = 375$ the turbulence is seen to be self-sustained as the region grows. The computations were here continued to $t = 160$ to verify the conclusion about self-sustained turbulence. At large times the spreading continues, but the elongation is less pronounced. Calculations were also carried out at $Re = 350$ in order to determine

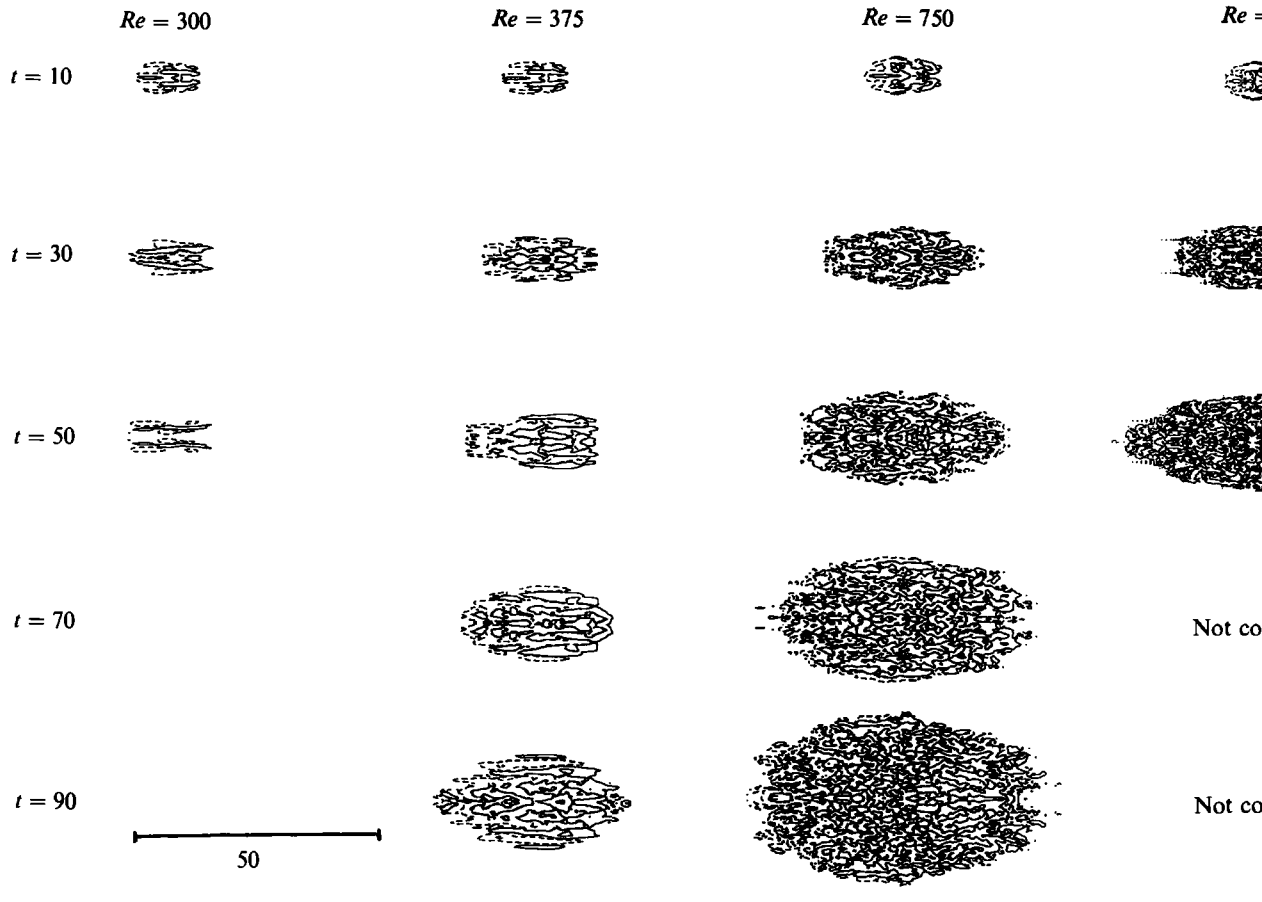

FIGURE 3. Spot development up to $t = 90$ for Reynolds numbers 300, 375 and 750, and up to $t = 50$ for $Re = 1500$. Cor
± 0.02 for the (x, z)-plane at $y = 0$ are shown. Dashed contours represent negative values in this and following figures. A l
given in the figure for reference (same in both directions).

this *critical* Reynolds number (Re_{crit}) within a narrow interval. The behaviour at this Reynolds number was found to be essentially identical to that at $Re = 300$, although here the decay was somewhat slower and the v-amplitudes had fallen below 0.02 at $t \approx 100$. Also the spanwise wavelength of the u-disturbance at large times was found to be about the same as for the lower Reynolds number. Hence, Re_{crit} is within the interval between 350 and 375, and from the behaviour at the higher value, it seems likely that Re_{crit} is close to 375. It does not seem meaningful to determine the critical value with greater accuracy.

The box size and number of modes used in the computations were chosen such that the spatial resolution at $Re = 750$ corresponded to a horizontal cell size of approximately 27×14 wall units, with the friction velocity, u_τ, taken from the central turbulent region of the spot. This is better than in the Poiseuille spot simulation of Henningson *et al.* (1987), and somewhat worse than in the well-verified simulations of turbulent channel flow at NASA Ames with two million modes (see Kim *et al.* 1987, p. 138). At both the higher Reynolds numbers the maximum cell size in the wall-normal direction was slightly above 5 wall units. For the spots at lower Reynolds numbers the resolution of course becomes correspondingly better. The temporal resolution was below 0.1 wall units for all cases.

The $Re = 1500$ spot in figure 3 was computed with twice the number of Chebyshev modes in a smaller box (90×40) giving nearly the same resolution in wall units as for $Re = 750$. The high-Reynolds-number computation was compared with a test run with the same box size and number of modes as for the lower Reynolds numbers. Although this represents a poor resolution in wall units the spot size at $t = 50$ was, within 5%, the same as for that in figure 3. Also spatially filtered r.m.s. levels (for definitions see §3.1) of the velocity fluctuations were the same within the uncertainty of the determination of these quantities. These are positive indications that the spatial resolution of the spots in figure 3 is sufficient to accurately determine shape, spreading rates, and turbulence statistics of the interior.

The oval shape of the spot is seen to be more accentuated at $Re = 1500$ than at 750 for the relatively early times over which the high-Re simulation was carried out. An interesting aspect is also whether the shape reaches a self-similar state. For this to be true the ratio between growth rates in the x- and z-directions should be equal to the length-to-width ratio. In order to investigate this aspect in more detail, and to further illustrate the contrast between the situation just above the critical Reynolds number ($Re = 375$) and that at $Re = 750$, the simulation for the latter was continued to $t = 160$. This could be achieved by restarting the field shown in figure 3 at $t = 90$ in a box with twice the extent in the two horizontal directions and twice the number of Fourier modes. Hence, identical spatial resolution as for earlier times was obtained by use of $512 \times 33 \times 512$ modes. The differences between the two Reynolds numbers shown in figure 4 are conspicuous and for the high-Re case the spot has become very large with a total length of the order of 100 half-gap widths. It is evident from figures 3 and 4 that the smallest scale in the turbulent region decreases with increasing Reynolds number, as expected. It was also found from analysis of the turbulent field that two-point correlations at large streamwise separations are substantially larger than for the corresponding channel flow. This was also observed experimentally in fully developed turbulent Couette flow by Robertson & Johnson (1970), and implies that the box-length requirement for simulations of the fully developed flow would be severe, and hence, that the number of modes needed for the description is significantly larger in this case than for channel flow at comparable Reynolds number and spatial resolution.

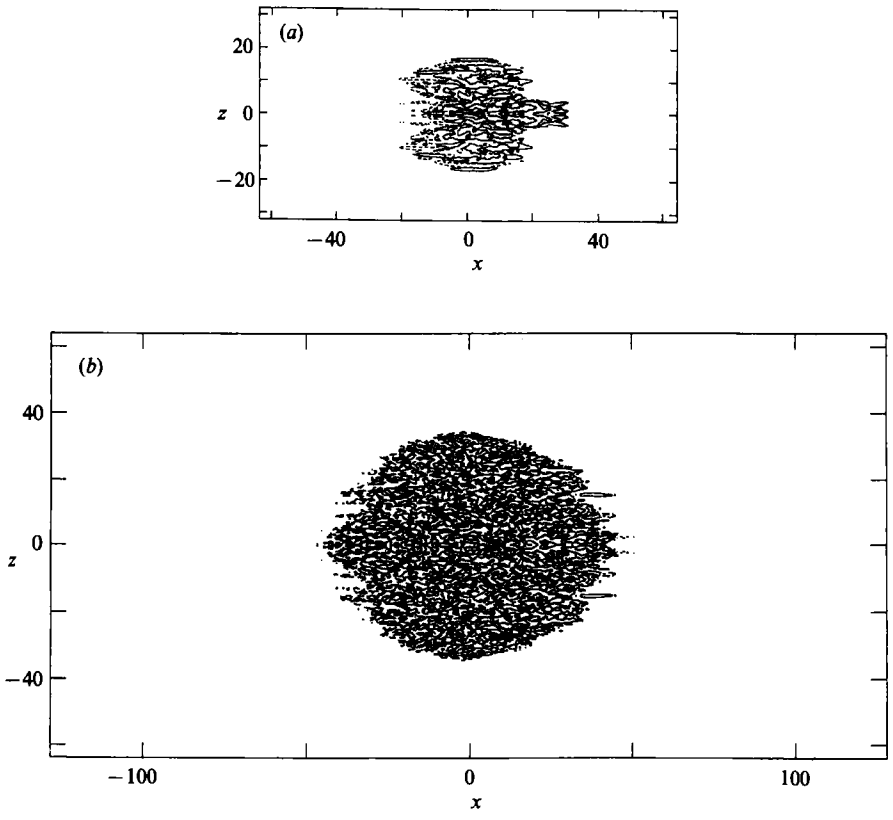

FIGURE 4. Contours (± 0.02) of v in the centreline (x, z)-plane at $t = 160$ for two different Reynolds numbers: (*a*) Re = 375 and (*b*) $Re = 750$.

From a comparison between figures 3 and 4 it is seen that the length-to-width ratio of the $Re = 750$ spot has decreased substantially between $t = 90$ and $t = 160$. A closer study of the shape development (figure 5*a–d*) shows that the growth-rate ratio is smaller than the length-to-width ratio throughout the development and is equal to unity within the uncertainty of determination at the latest times. This implies that the half-length, L, to half-width, W, ratio, which is 2.2 at $t = 50$ and 1.4 at $t = 160$, slowly tends to unity (see figure 5*d*). Hence, there is a slow approach towards a circular shape.

The variation of the half-length up to moderate times shows clearly, in figure 5(*a*), that the streamwise spreading rate increases with increasing Reynolds number over the range investigated here. The results in figure 5 (*b*), on the other hand, indicate that the spanwise growth rate levels off, and is approximately the same at the two highest Reynolds numbers. At $Re = 750$ the rate of spread in the spanwise direction is $0.23U_0$. This can be translated into a spreading half-angle of approximately 13° for the case with one of the walls stationary, where the uncertainty corresponds to approximately $\pm 0.5°$ (as estimated from the scatter in the growth-rate data in figure 5). This spreading rate is roughly twice that at half the Reynolds number, but approximately the same as for $Re = 1500$. This should be compared with the corresponding behaviour in other shear flows. In boundary layers a spreading half-angle of about 10° is found to be relatively independent of Reynolds number (see e.g. Wygnanski, Zilberman & Haritonidis 1982). However, in both plane Poiseuille flow

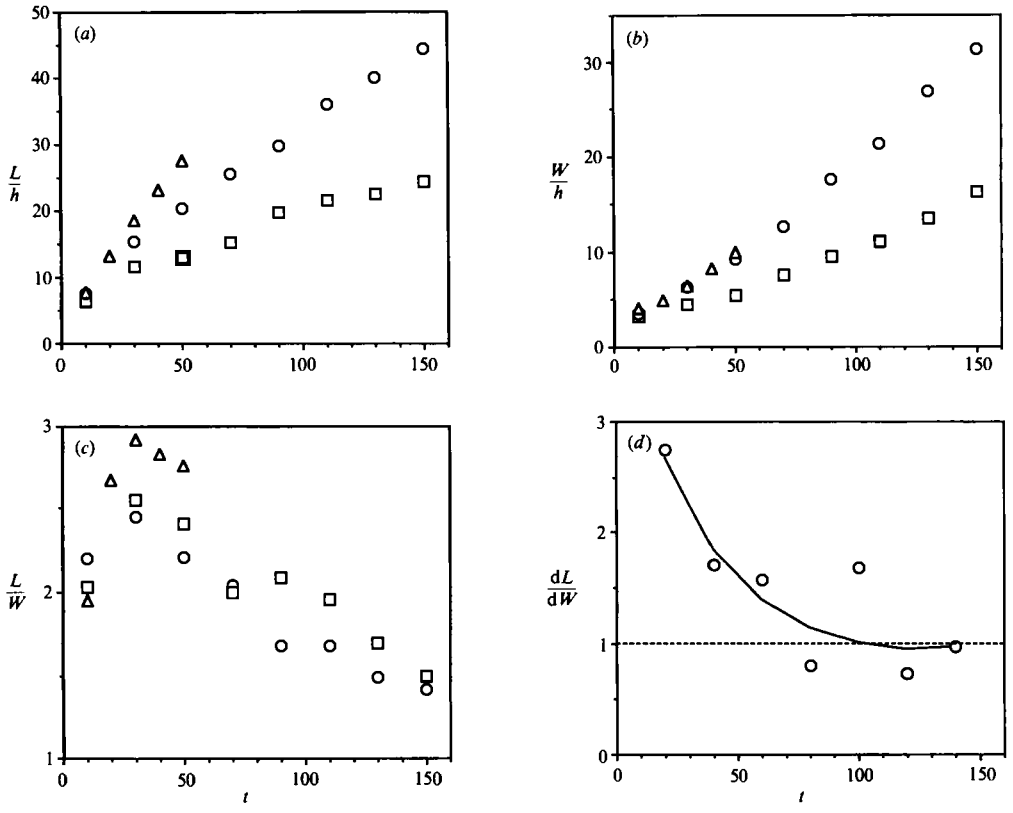

FIGURE 5. Spot spreading characteristics as function of time for $Re = 375$ (□), $Re = 750$ (○) and $Re = 1500$ (△). (*a*) Half-length L, (*b*) half-width W, (*c*) aspect ratio L/W and (*d*) growth-rate ratio dL/dW.

(Henningson & Alfredsson 1987) and free-surface water-table flow (Lindberg *et al.* 1984) an increasing trend with increasing Reynolds number has been observed. In the latter case the spreading angle levelled off in a manner similar to that observed here for the Couette spot.

An interesting feature of the spreading of the spot, which to some extent may be seen from figure 5(*b*) and is evident from closer inspection of the data, is that the spanwise growth first reaches a fairly constant level after some time, and that this level is considerably higher than that at small times. A *virtual origin* would hence be displaced downstream owing to this effect, which indicates that the mechanism for the spanwise spreading first attains its full strength when the spot has become large enough. A natural coupling would be to the modification and possible destabilization of the surrounding laminar velocity field (Gad el Hak, Blackwelder & Riley 1981). This modification is caused by the partial flow blockage resulting from the higher wall friction in the interior of the spot, and the spot growth. This effect diverges the streamlines around the turbulent region. The downstream displacement of the virtual origin is also present in the simulations of a Poiseuille spot (Henningson *et al.* 1987).

The spreading characteristics shown in figure 5 pertain to the case of an initial disturbance with spanwise symmetry (around the $z = 0$ plane). It is known from experimental investigations in various flows that spot characteristics are largely

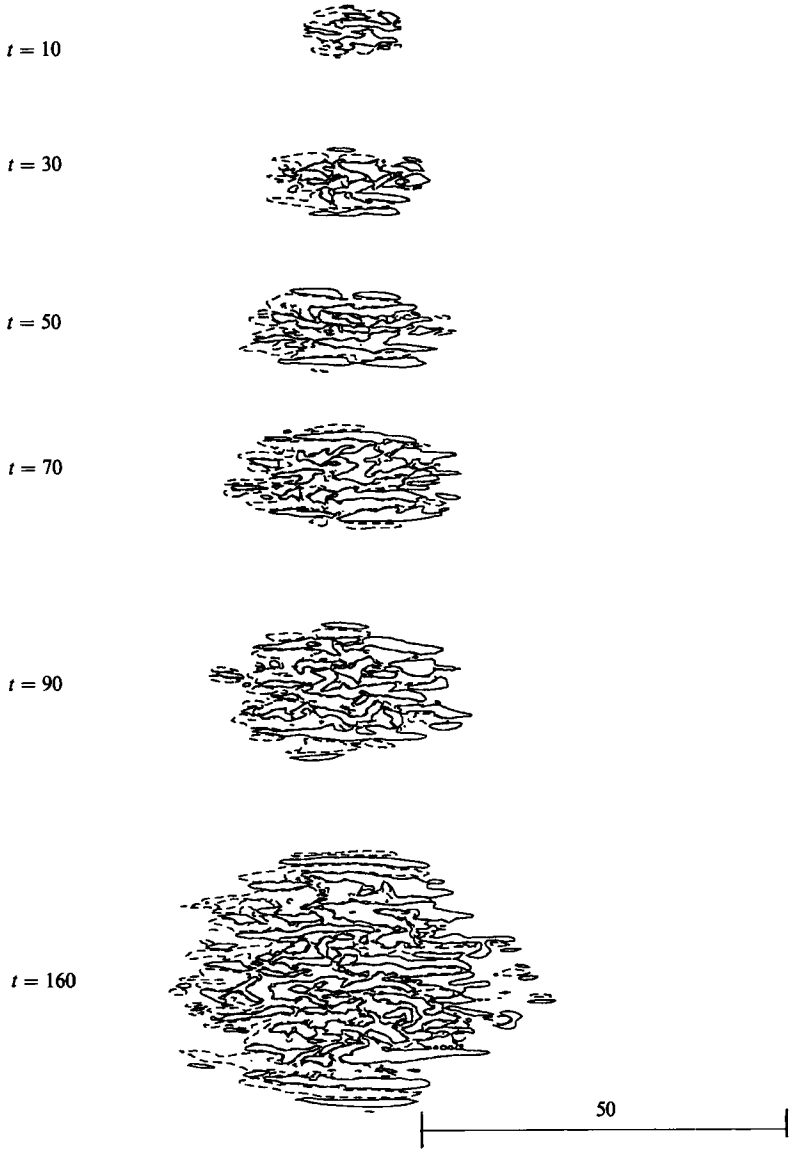

FIGURE 6. Development of the spot for $Re = 375$ originating from an initial disturbance without spanwise symmetry ($\theta = 10°$, see figure 2). Contours of v at ± 0.02 for the (x, z)-plane at $y = 0$ are shown. A lengthscale is given in the figure for reference (same in both directions).

insensitive to the specifics of the initial disturbance if it is of sufficiently high amplitude. One could possibly expect a more accentuated sensitivity for Reynolds numbers close to the critical value. To investigate this issue and the possibility that initial asymmetries become strongly amplified, a test run without the symmetry constraint was performed for $Re = 375$ with an initial disturbance rotated by 10° around the $x = z = 0$ line (see figure 2). This implies a major change of the initial disturbance and also introduces an initial u-component. The spot development for this case is shown in figure 6 for times up to 160. It is seen that the initial spanwise asymmetry has no tendency to be amplified. On the contrary, the overall characteristics tend to become more and more similar to the symmetric spot. The size

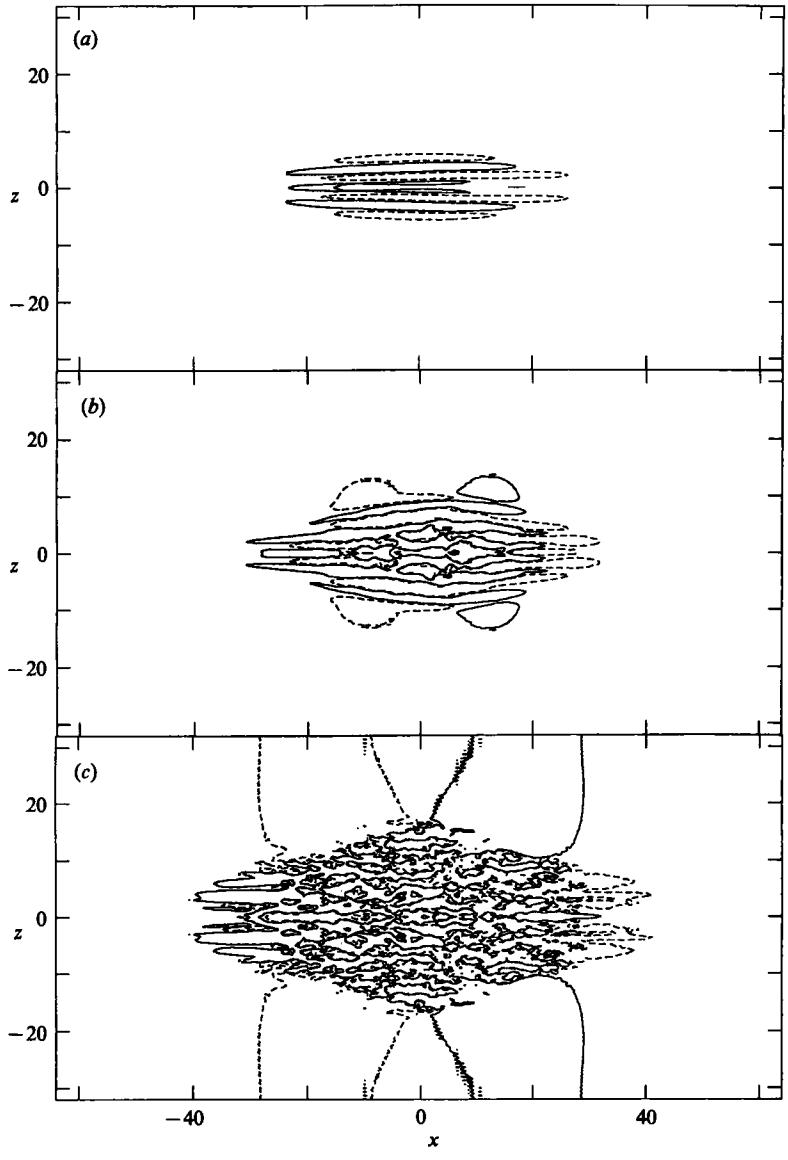

FIGURE 7. Streamwise velocity disturbance part of the spot at $t = 90$ for (*a*) $Re = 300$, (*b*) $Re = 375$ and (*c*) $Re = 750$. Contours at ± 0.05 are shown.

of the asymmetric spot, at $t = 160$, is within 5% of the symmetric one. Thus, it appears sufficient to study symmetric cases in order to determine all essential characteristics of the Couette spot.

For both the symmetric (figure 4*a*) and the asymmetric (figure 6) spots at $Re = 375$ a pattern with longitudinal streaks can be observed at the spanwise edge of the spot. This streaky or wave-like pattern also contains a significant w component, and was found to become somewhat more pronounced as the computation was pursued further to $t = 200$ for the asymmetric case. It bears some resemblance to the wave packet observed at the wing tips of Poiseuille spots. However, the streaky pattern becomes less distinct at higher Reynolds numbers (see

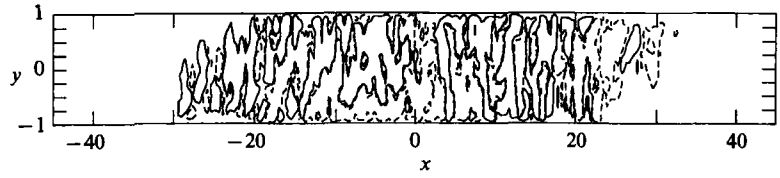

FIGURE 8. Contours (± 0.02) of v in the mid (x, y)-plane at $t = 50$ ($Re = 1500$).

figure 4*b*). It could be observed that the streaks move outward with a velocity slightly lower than the spreading rate of the turbulent region. Consequently they are not phase locked to the spot, but new streaks are generated outside the spot and are subsequently overtaken by it.

The streamwise velocity disturbance at the centreline is shown in figure 7 for various Reynolds numbers. The four lobes outside the turbulent region indicate the areas mostly affected in the external flow, and are present for all Reynolds numbers for which turbulence can be sustained. From analysis of the data one finds that the velocity field outside the spot is essentially two-dimensional in that it lacks a significant vertical component. The oscillations in the z-direction seen at $Re = 750$ are of numerical origin, but are of very small amplitude, and become visible here owing to the small gradients in that region.

Close to the moving walls the spot extends further in the respective direction than is seen in figure 3. Thus, in the reference frame of, say, the *lower* wall, we may say that there is an overhang in the downstream direction close to the *upper* wall (figure 8). This is somewhat similar to the boundary-layer spot, although there is a free stream above the overhang in that case. If one were to compare with a flow visualization experiment, with e.g. platelet particles, the streamwise half-extent of the visualized turbulent region would be 4–5 units larger than the values given in figure 5(*a*) (except for very short times) because of the overhang. Hence, for large enough times it would not affect the estimated streamwise spreading rate.

In order to enable meaningful comparisons with other types of flows the total streamwise spreading rate should be divided by two since the overall velocity difference here is 2.0 and not 1.0 as in boundary-layer and Poiseuille flows. Hence, an appropriate measure is the rate of increase of the half-length, $\mathrm{d}L/\mathrm{d}t$, which (from figure 5*a*) for $Re = 750$ can be found to be close to 0.4 at early times, decreasing to about 0.24 (± 0.02) at $t = 160$. This may be compared with e.g. the difference between leading- and trailing-edge velocities of the boundary-layer spot, which is about 0.4. The corresponding value for the Poiseuille spot is close to the Couette value (see Henningson *et al.* 1987).

3.1. *Turbulence statistics through spatial filtering*

In experimental situations the average flow field of the spot and turbulence statistics in the interior are evaluated by use of ensemble averaging over a large number of spots. This is of course not a feasible technique in simulations. Mean flow quantities and turbulence statistics can still be determined within a reasonable accuracy by spatial filtering or averaging techniques. In the present study, a spatial filter with a Gaussian hat filter function was used, and various values of the filter lengthscale were tested. The results were found to be rather insensitive to the choice of this lengthscale. The following results all represent the $Re = 750$ case, but are similar at the other Reynolds numbers.

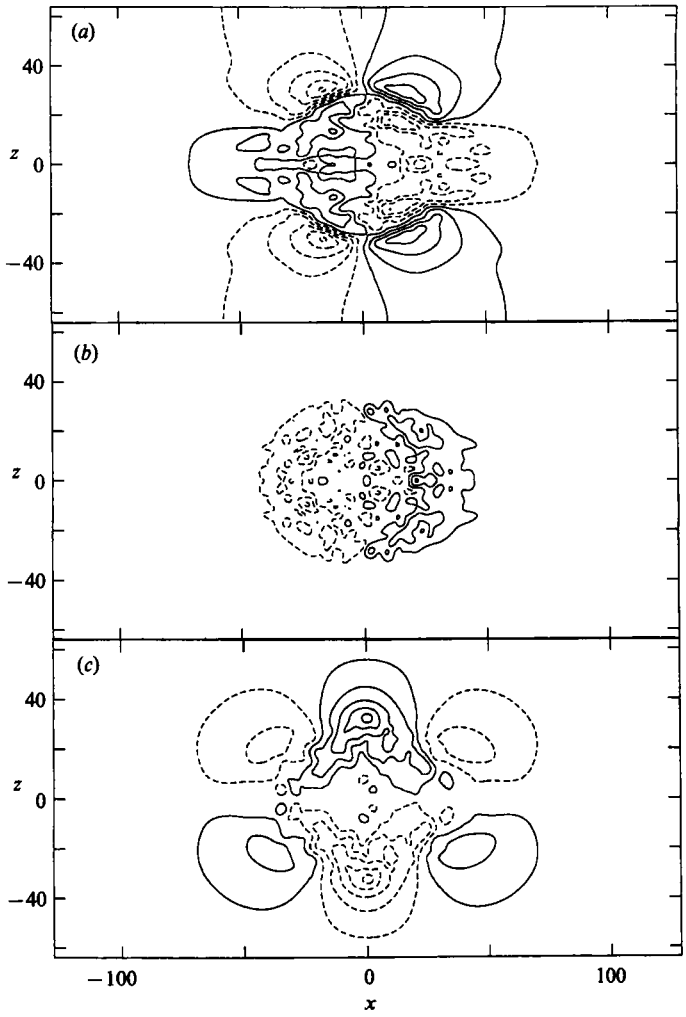

FIGURE 9. Spatially low-pass filtered spot at $t = 160$ ($Re = 750$). (*a*) Filtered u-field with contours starting at -0.225 and a contour increment of 0.05, (*b*) filtered v-field with contours starting at -0.025 and increment 0.01, (*c*) filtered w-field with contours starting at -0.225 and increment 0.05.

Spatially filtered mean values were obtained by use of a Gaussian low-pass filter in wavenumber space. Figure 9 (*a–c*) shows the *average* u, v and w fields (denoted by angle brackets) as determined by

$$\langle \hat{u} \rangle(\alpha, \beta) = \hat{u}(\alpha, \beta)\, \mathrm{e}^{-(k/\frac{1}{8}\pi)^2},$$

where $k = (\alpha^2 + \beta^2)^{\frac{1}{2}}$ is the total horizontal wavenumber, and $\hat{u}$ is the two-dimensional Fourier transform of u. In physical space this corresponds to

$$\langle u \rangle = \tfrac{1}{8}\pi^2 \int\int u(x+\xi, z+\zeta)\, \mathrm{e}^{-[r/(8/\pi)]^2}\, \mathrm{d}\xi\, \mathrm{d}\zeta,$$

where $r = (\xi^2 + \zeta^2)^{\frac{1}{2}}$. Hence, in this case the diameter of the circle that corresponds to a filter function larger than 1/e is $16/\pi$, i.e. approximately 5 half-heights or 270 wall units. This may be compared with the spot width, which at $t = 160$, $Re = 750$ is about 69 half-heights.

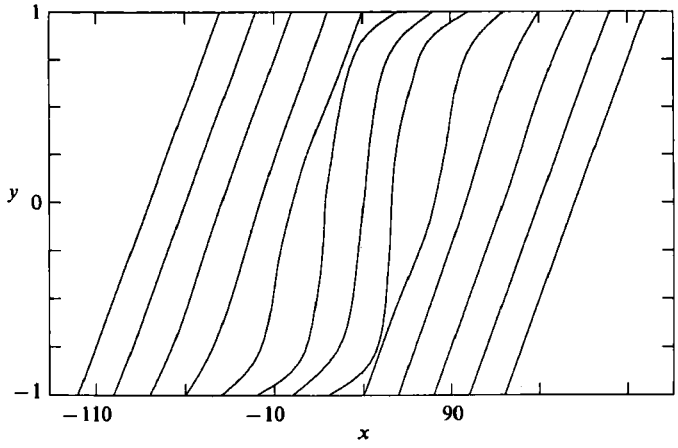

FIGURE 10. Filtered velocity profiles in the mid (x, y)-plane ($t = 160$, $Re = 750$) for various streamwise locations through the spot. The intersection of the profile with the abscissa represents the actual x-location of the respective profile. ($\Delta x = 40 \Leftrightarrow \Delta u = 1$).

Despite the fact that the centreline plane shown here is stationary with regard to the spot development, there is a weak overall flow structure inside and outside the spot. In the rear half of the interior there is a flow towards the lower surface, which is balanced by an upward flow in the forward part. This is a natural consequence of the higher wall friction in the interior as compared to the surrounding flow. The interior *mean* flow, though, becomes weaker as the spot grows. Here, and in the following figures the flow field at $t = 160$ ($Re = 750$) is used for the analysis to give a turbulent area as large as possible.

The modification of the external flow now stands out in a clear way as the turbulent fluctuations of the interior are filtered out, and the extremum points of the four lobes for u were found to be just at the laminar–turbulent interface. The u-velocity is as large as 0.22 just outside the turbulent region, whereas the laminar Couette value is zero. It is seen that the modified external flow is totally dominated by the horizontal components, and that there is a motion out from the spot near the midpoint, $x = 0$, contrasted with motion towards the spot at the leading and trailing parts.

By construction of filtered fields it was also possible to determine local *average* velocity profiles throughout the spot. The profiles at the mid (x, y)-plane, shown in figure 10, exhibit the typical s-shape of turbulent Couette profiles for the position in the centre region.

The fluctuating velocity field, from which turbulence statistics were computed, was constructed simply as the difference between the total field and the spatially averaged, or filtered one. The resulting fluctuating part of u (figure 11) has a structure quite similar to the v-field (cf. figure 4*b*). To construct turbulence intensities the fluctuating parts were squared, whereafter the same filter as above was applied to obtain mean-square values. Contours of the r.m.s. levels of u and v at the centreline and at a position ($y = -0.707$) that corresponds to a distance from the lower wall of 16 wall units, are shown in figure 12. The latter position is hence in the region of expected maximum streamwise turbulence intensity.

The intensities are significantly higher near the periphery of the spot (i.e. near the laminar–turbulent interface) than in the central part. This feature, which could also be observed by plotting spanwise cuts through the unfiltered velocity fields, is also

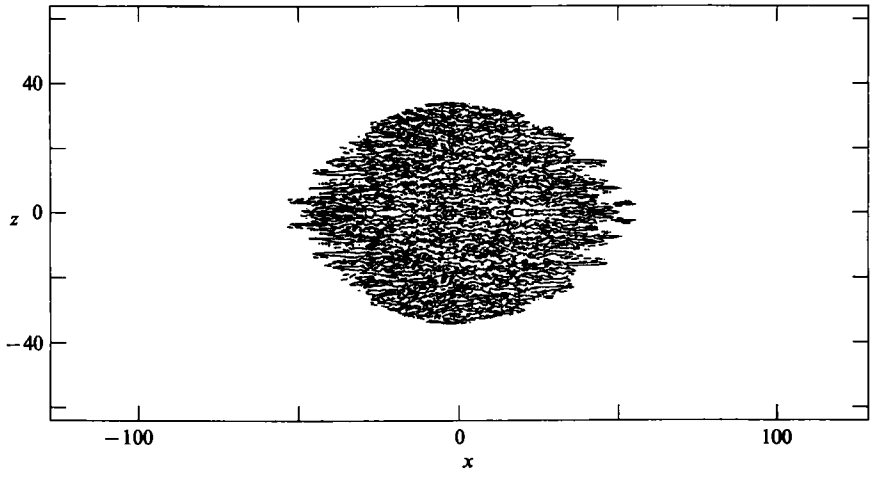

FIGURE 11. Fluctuating part of the u-field (total minus spatially filtered field) at $t = 160$ ($Re = 750$). Contours at ± 0.05 are shown.

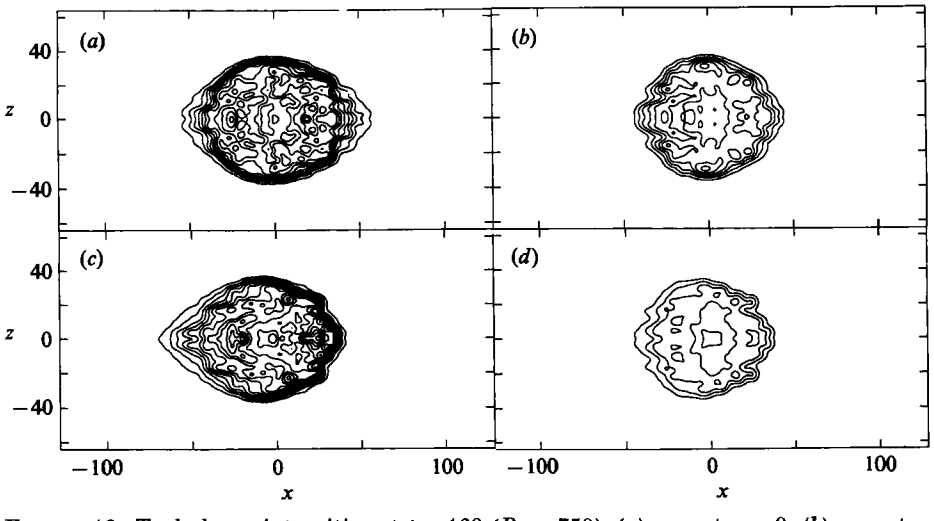

FIGURE 12. Turbulence intensities at $t = 160$ ($Re = 750$). (*a*) $u_{\rm rms}$ at $y = 0$, (*b*) $v_{\rm rms}$ at $y = 0$, (*c*) $u_{\rm rms}$ at $y = -0.707$, (*d*) $v_{\rm rms}$ at $y = -0.707$. Contour increment is 0.02.

present for the v-fluctuations. At the near-wall position we note that the asymmetry is considerably more accentuated for the u-component. The maximum local $u_{\rm rms}$ there corresponds to approximately $3.7\,u_\tau$. In the central part typical values are around $2.3\,u_\tau$. These values should be compared with the maximum $u_{\rm rms}/u_\tau$ found in the near-wall region of turbulent shear flows, which is 2.8–2.9. The v-intensities are about a factor of 2.5 smaller.

Smaller details of the contours in figure 12 should not be regarded as significant, but maximum and typical levels are, as could be verified from comparisons with the opposite near-wall position (at $y = +0.707$).

To obtain profiles of the turbulence intensities averaged over a large part of the central region of the spot, one can apply the above filter with a larger filter scale when constructing the mean-square values. Figure 13 shows the distributions of $u_{\rm rms}/u_\tau$

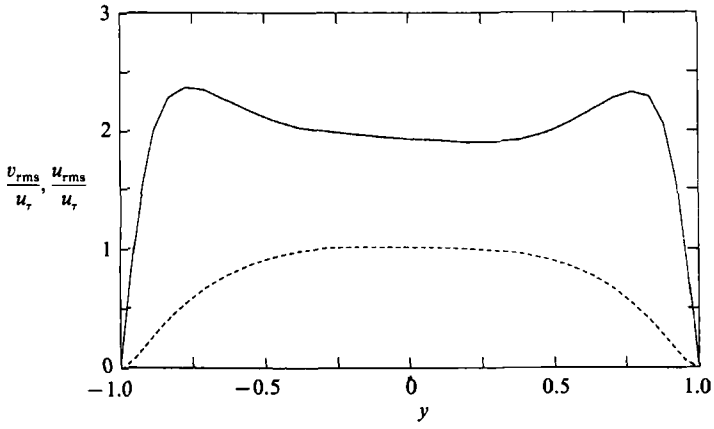

FIGURE 13. Turbulence intensities, u_{rms}/u_τ (—), and v_{rms}/u_τ at $t = 160$ ($Re = 750$) as function of y. The intensities were here averaged over a large part of the central region of the spot.

and v_{rms}/u_τ averaged with a filter such that the 1/e diameter corresponds to 19 half-heights. The differences between the two opposite sides illustrate the uncertainties associated with the values. The maximum of u_{rms}/u_τ is about 2.4, and is found at $y^+ \approx 12$, whereas the v-intensity at this low Reynolds number has its maximum level at the centreline. These data also yield that the relative turbulence level u_{rms}/u_{mean} reaches its highest level at the surfaces, where it is 0.41 (± 0.02). This is in close agreement with the experimental results of Alfredsson *et al.* (1988) obtained both in boundary layers and channel flows, as well as with the simulation results of Gilbert (1988), but is slightly higher than the simulation result of Kim *et al.* (1987).

The fluctuation intensities of u on the centreline are typically around $1.9\,u_\tau$, and hence only about 20% lower than at the near-wall position. For the $Re = 375$ spot typical values of u_{rms}/u_τ at the centreline are even higher (about 2.6). This is in contrast to e.g. high Reynolds-number turbulent channel flow, where the centreline u-intensity is about $0.9\,u_\tau$ (Johansson & Alfredsson 1982). One should bear in mind though that this is a turbulent flow at extremely low Reynolds number. The lowest Reynolds number, Re_τ, based on half-channel width and friction velocity, for which fully developed turbulent channel flow can be sustained is about 150. This Reynolds number is also the half-channel width in wall units. For the fields shown in figure 12, Re_τ is as low as 54.

The low Reynolds number is one reason for the high value of u_{rms} at the centreline and the relatively small difference between the centre and the maximum levels near the wall. A further reason is the fact that for Couette flow, in contrast to e.g. channel flow, the mean velocity gradient is non-zero at the centreline. This also implies a non-zero turbulence production there. This gives a significant effect at the low Reynolds number of the spot analysed here. Actually it will persist also at higher Reynolds numbers since the gradient at $y = 0$ decreases quite slowly. For the present spot ($Re = 750$) this gradient varies between $0.25U_0/h$ and $0.35U_0/h$ in the turbulent part at $y = 0$. It may here be worthwhile to note that measured values of u_{rms}/u_τ (Robertson & Johnson 1970) at the centreline of fully developed turbulent Couette flow ($Re = 7\text{–}16 \times 10^3$) are about 1.5.

4. Summary and conclusions

The lowest Reynolds number for which Couette spots can be sustained has here been determined within a narrow interval, and found to be slightly below 375. The horizontal extent of the spot has an elliptical character, with an aspect ratio that increases with increasing Reynolds number. The streamwise elongation becomes less pronounced with increasing time though, and there is a slow approach towards a circular shape.

The spanwise growth was found to increase with increasing Re for low Reynolds numbers, but levelled off to a constant rate at high Re. In the reference frame of one of the solid surfaces this spreading rate can be translated into a spreading half-angle of 13° for the Couette spot at high Reynolds numbers. This is hence a more rapid spreading than for boundary-layer spots.

The overhang, as seen from vertical cuts of the spot, and the zero curvature of the velocity profile at the wall resemble the zero-pressure-gradient boundary-layer case. The Couette spot, hence, constitutes an interesting case that may, in some sense, be regarded as intermediate between the Poiseuille and boundary-layer spots.

Spatial filtering of the velocity fields showed that the modifications of the horizontal components of the laminar flow surrounding the spot are quite large just outside the turbulent region. This opens possibilities for future investigations of possible destabilization of the surrounding flow.

Determination of turbulence characteristics (through spatial filtering) showed that the combination of low Reynolds number and the presence of mean shear at the centreline gives a relatively small difference in u_{rms} between the centreline and near-wall positions. In contrast, the turbulence intensity distributions close to the walls are remarkably similar to those in high-Reynolds-number flows. It is here noteworthy that Re_τ for Couette flow can be as low as 29 in a growing spot.

Since no corresponding experimental results exist today this study represents a true prediction of the basic features of turbulent spots in plane Couette flow.

This research has been partially sponsored by the Swedish State Board for Technical Development, the Aeronautical Institute of Sweden and The Göran Gustafsson Foundation. CRAY-time has been granted from the Swedish National Supercomputer Center. We also wish to thank Henrik Alfredsson for many fruitful discussions on the present topic and Dan Henningson for cooperation with the writing of the simulation code.

REFERENCES

Alfredsson, P. H., Johansson, A. V., Haritonidis, J. H. & Eckelmann, H. 1988 On the fluctuating wall shear stress and velocity field in the viscous sublayer. *Phys. Fluids* **31**, 1026.

Breuer, K. S. 1989 Evolution of localized disturbances in laminar boundary layers. In *Proc. Third IUTAM Symp. on Laminar Turbulent Transition, Toulouse, Sept. 1989*.

Ellingsen, T., Gjevik, B. & Palm, E. 1970 On the non-linear stability of plane Couette flow. *J. Fluid Mech.* **40**, 97.

Gad el Hak, M., Blackwelder, R. F. & Riley, J. J. 1981 On the growth of turbulent regions in laminar boundary layers. *J. Fluid Mech.* **110**, 73.

Gallagher, A. P. 1974 On the behaviour of small disturbances in plane Couette flow. Part 3. The phenomenon of mode-pairing. *J. Fluid Mech.* **65**, 29.

Gilbert, N. 1988 Numerische Simulation der Transition von der laminaren in die turbulente Kanalströmung. Ph.D. Thesis, Fakultät für Maschinenbau der Universität Karlsruhe.

GREENGAARD, L. 1988 Spectral integration and two-point boundary value problems. *Research Rep.* YALEU/DCS/RR-646, Dept. of Comp. Science, Yale University.

HENNINGSON, D. S. & ALFREDSSON, P. H. 1987 The wave structure of turbulent spots in plane Poiseuille flow. *J. Fluid Mech.* **178**, 405.

HENNINGSON, D. S., JOHANSSON, A. V. & LUNDBLADH, A. 1989 On the evolution of localized disturbances in laminar shear flows. In *Proc. Third IUTAM Symp. on Laminar Turbulent Transition, Toulouse, Sept. 1989.*

HENNINGSON, D. S., SPALART, P. & KIM, J. 1987 Numerical simulations of turbulent spots in plane Poiseuille and boundary layer flows. *Phys. Fluids* **30**, 2914–2917.

JOHANSSON, A. V. & ALFREDSSON, P. H. 1982 On the structure of turbulent channel flow *J. Fluid Mech.* **122**, 295.

KIM, J., MOIN, P. & MOSER, R. 1987 Turbulence statistics in fully developed channel flow at low Reynolds number. *J. Fluid Mech.* **177**, 133.

LEUTHEUSSER, H. J. & CHU, V. H. 1971 Experiments on plane Couette flow. *J. Hydraul. Div. ASCE* **97**, 1269.

LINDBERG, P. A., FAHLGREN, E. M., ALFREDSSON, P. H. & JOHANSSON, A. V. 1984 An experimental study of the structure and spreading of turbulent spots. *Proc Second IUTAM Symp. on Laminar Turbulent Transition, Novosibirsk*, pp. 617–624. Springer.

NAGATA, M. 1990 Three-dimensional finite-amplitude solutions in plane Couette flow: bifurcation from infinity. *J. Fluid Mech.* **217**, 519.

ORSZAG, S. A. & KELLS, L. C. 1980 Transition to turbulence in plane Poiseuille and plane Couette flow. *J. Fluid Mech.* **96**, 159.

REICHARDT, H. 1956 Über die Geschwindigkeitsverteilung in einer geradlinigen turbulenten Couetteströmung. *Z. Angew. Math. Mech.* Sonderheft 26.

RILEY, J. J. & GAD-EL-HAK, M. 1985 The dynamics of turbulent spots. In *Frontiers in Fluid Mechanics* (ed. S. H. Davis & J. L. Lumley), pp. 123–155. Springer.

ROBERTSON, J. M. & JOHNSON, H. F. 1970 Turbulence structure in plane Couette flow. *J. Enging Mech. Div. ASCE* **96** (EM6), 1171.

SPALART, P. R. & YANG, K. 1987 Numerical study of ribbon-induced transition in Blasius flow. *J. Fluid Mech.* **178**, 345.

WYGNANSKI, I., ZILBERMAN, M. & HARITONIDIS, J. H. 1982 On the spreading of a turbulent spot in the absence of a pressure gradient. *J. Fluid Mech.* **123**, 69.